NASA TECHNICAL NOTE

NASA TN D-2687

NASA TN D-2687

TURBULENT SKIN FRICTION AT HIGH REYNOLDS NUMBERS AND LOW SUPERSONIC VELOCITIES

by Mary W. Jackson, K. R. Czarnecki, and William J. Monta

Langley Research Center
Langley Station, Hampton, Va.

NATIONAL AERONAUTICS AND SPACE ADMINISTRATION • WASHINGTON, D. C. • MARCH 1965

TURBULENT SKIN FRICTION AT HIGH REYNOLDS NUMBERS AND LOW SUPERSONIC VELOCITIES

By Mary W. Jackson, K. R. Czarnecki, and William J. Monta

Langley Research Center
Langley Station, Hampton, Va.

NATIONAL AERONAUTICS AND SPACE ADMINISTRATION

For sale by the Office of Technical Services, Department of Commerce, Washington, D.C. 20230 -- Price $2.00

TURBULENT SKIN FRICTION AT HIGH REYNOLDS NUMBERS AND LOW SUPERSONIC VELOCITIES

By Mary W. Jackson, K. R. Czarnecki,
and William J. Monta
Langley Research Center

SUMMARY

An investigation has been made to gather experimental skin-friction data over a wide range of high Reynolds numbers at low supersonic velocities. Tests were conducted at Mach numbers 1.61 and 2.20 over a tunnel range of Reynolds number per foot from 0.8×10^6 to 8.0×10^6. Test data were obtained from boundary-layer local skin-friction measurements and boundary-layer momentum surveys at five tunnel-wall measurement stations.

The results indicate that the effective Reynolds number of the turbulent boundary layer ranges from about 7×10^6 to 150×10^6 at Mach numbers 1.61 and 2.20. The experimental average skin-friction coefficients and the experimental local skin-friction coefficients for this range are in agreement with the levels of the Sommer and Short T', the Monaghan T', the Eckert T', the Cope and Monaghan, the Wilson and Van Driest theoretical curves. The variation of the average skin-friction coefficient and the local skin-friction coefficient with effective Reynolds number tends to follow the theoretical predictions at the test Mach numbers.

INTRODUCTION

In order to approach optimum design and to evaluate the performance of long-range supersonic aircraft, reliable estimates of airplane drag must be made. Since skin-friction drag comprises a large part of the total airplane drag, it is imperative that accurate methods of predicting turbulent skin-friction drag be known. A number of theoretical or theoretical-empirical approaches have been developed. Examinations of experimental data available for verification of the various theories indicate that: (1) the bulk of such data falls in the Reynolds number range below 20×10^6, (2) that there is only a limited amount of data in the Reynolds number range from 20×10^6 to 100×10^6, and (3) virtually no data fall in the range above 100×10^6 which might be applicable to long-range supersonic vehicles. The present state of the art indicates a need for accurate experimental data in the Reynolds number range above 100×10^6. Lack of such data has hindered the proof of

adequacy of the existing theories in this range and the choice of the best approach to make in extrapolating the low Reynolds number data to this desired range.

The present investigation was undertaken to gather experimental skin-friction data at high Reynolds numbers and low supersonic velocities. This investigation was conducted in two phases: local skin-friction measurement tests, and boundary-layer surveys. Tests were conducted at five stations on the sidewall of the Langley 4- by 4-foot supersonic pressure tunnel at Mach numbers of 1.61 and 2.20. In order to obtain the widest possible Reynolds number variation, tests were conducted over the range of maximum Reynolds number per foot for the tunnel. The unit Reynolds numbers varied for the test from about 0.8×10^6 to about 8.0×10^6. All tests were conducted under essentially zero heat-transfer conditions.

SYMBOLS

C_F	average skin-friction coefficient
C_f	local skin-friction coefficient
C_p	pressure coefficient
D	friction drag
M	Mach number
p	static pressure
$p_{t,1}$	free-stream stagnation pressure
$p_{t,2}$	pitot pressure
q	dynamic pressure
R	free-stream Reynolds number
R_x	Reynolds number based on free-stream conditions and axial distance from virtual origin of turbulent boundary layer
S	disk area
T'	reference temperature
u	local velocity
u_δ	local velocity just outside boundary layer

x	axial distance from virtual origin of turbulent boundary layer
x'	axial distance from tunnel first minimum
y	vertical distance from wall
δ	boundary-layer thickness
θ	boundary-layer momentum thickness
ρ	local density
ρ_δ	local density just outside boundary layer
μ	Mach angle

APPARATUS AND METHODS

Wind Tunnel

This investigation was conducted in the Langley 4- by 4-foot supersonic pressure tunnel, which is a rectangular, closed-throat, single-return wind tunnel with provisions for the control of pressure, temperature, and humidity of the enclosed air. Flexible nozzle walls were adjusted to give the desired test-section Mach numbers of 1.61 and 2.20. During the tests, the dewpoint was kept below -20° F to insure negligible effects of water condensation in the supersonic nozzle.

Instrumentation

Skin-friction balance.- The skin-friction balances used in this investigation were built by the Defense Research Laboratory of the University of Texas for another investigation and loaned to NASA for this investigation. The balances and techniques for using them are fully described in reference 1. The balances were of the floating-element type, having a 1-inch-diameter disk and an annular gap around the disk of 0.005 inch. A schematic drawing of a typical floating-element balance is given in figure 1. The air stream exerts a shearing force on the disk which is suspended by two fixed-end leaf-spring flexures. The position of the core which duplicates the motion of the disk determines the electrical output of the differential transformer. The electrical output of the transformer is therefore a direct function of the shearing force felt by the disk. Proper calibration of the balances correlated the disk-surface shear and the voltage output. Balances were calibrated both on the bench before testing and in the tunnel, before and after each run.

Inside and outside wall temperatures close to the balances were measured with iron-constantan thermocouples and the measurements were recorded on a potentiometer.

Boundary-layer probe and mechanism.- The boundary-layer probe and mechanism are shown in figure 2. The momentum surveys were made by using a 0.050-inch-outside-diameter stainless-steel probe flattened and honed to give an opening approximately 0.003 inch high. The wall thickness at the tip was about 0.003 inch.

The probe was remotely controlled from outside the tunnel wall by a micrometer-type screw, which permitted travel in the direction normal to the wall only. The dial indicator was graduated in 0.001-inch increments and probe positioning could be controlled to the nearest 0.0005 inch. Pressures were measured with differential pressure transducers and recorded. The total-head pressure and wall static pressure were measured during the same run.

Tests and Test Procedures

Tests were conducted in two major phases: boundary-layer local-skin-friction measurements and boundary-layer momentum surveys. All tests were conducted on the tunnel sidewall within the constant Mach number area of the tunnel test section. Nominal locations of the five measurement stations for both phases are given in figure 3 in feet. Data were obtained at free-stream Mach numbers of 1.61 and 2.20 over a range of tunnel stagnation pressures from about 430 to about 4300 pounds per square foot which correspond to tunnel Reynolds numbers per foot of about 0.8×10^6 to 8.0×10^6. The tunnel stagnation temperature was held constant for a given pressure and varied from about 100° F to 120° F throughout the test program.

Test procedure for both phases of the testing consisted of starting at the low tunnel stagnation pressures and advancing to higher pressures. Whenever data were to be taken, the tunnel was brought to and held at the desired test condition. In each test run, a repeat was made of some point to serve as a checkpoint. During the skin-friction balance tests, the balances at the various stations were interchanged. Drag indications were recorded as voltage output of the servomechanism. Inside and outside wall temperatures were also recorded.

For each boundary-layer total pressure survey an average of 30 readings was taken. Survey measurements extended from the wall to outside the boundary layer as determined by several readings.

Data Reduction

The local skin-friction coefficients were calculated from the relationship

$$C_f = \frac{D}{qS}$$

where drag force D was measured directly on the skin-friction elements. Dynamic pressure q was calculated from free-stream conditions and area S was the area of the disk.

In reducing the pressure data from the boundary-layer probe survey, it was assumed (1) that the stagnation temperature throughout the boundary layer was constant and equal to the measured free-stream stagnation temperature, and (2) that the static pressure was constant and equal to that measured at the wall. The data were reduced to momentum thickness θ with the following relationship

$$\theta = \int_0^{\delta} \frac{\rho u}{\rho_\delta u_\delta}\left(1 - \frac{u}{u_\delta}\right)dy$$

Local conditions of density and velocity outside the boundary layer were used as reference values. Examination of the variation of typical experimental C_p (measured at the wall) with x' shown in figure 4, in general, indicate uniformity of static pressures at the five stations with the possible exception of a dip in C_p at stations 3 and 4 ($M = 2.20$). Local Mach numbers based on ratios of wall static pressure to tunnel stagnation pressure ahead of the shock $p/p_{t,1}$ (method 1) are presented in figure 5, and local Mach numbers based on the ratios of total pressure measured by the total-pressure probe just outside the boundary layer to tunnel stagnation pressure $p_{t,2}/p_{t,1}$ (method 2) are presented in figure 6. As expected, the data of figure 5 exhibit a dip at stations 3 and 4 ($M = 2.20$). Data of figure 6 do not indicate the dip shown in figures 4 and 5 and thereby suggest the possibility that the variation in C_p at stations 3 and 4 ($M = 2.20$) is due to orifice-installation error. The Mach numbers computed by method 2 (fig. 6) appear to be somewhat higher than those computed by method 1 (fig. 5) and indicate a possible loss of total pressure from the settling chamber to the measurement stations. In general, the free-stream center-line Mach number values lie somewhere between the two sets of computed Mach numbers.

The virtual origin of the turbulent boundary layer was established by using the technique described by Peterson in reference 2. This technique employs local skin-friction coefficients and Reynolds numbers based on momentum thickness.

Average skin-friction coefficients were calculated from

$$C_F = \frac{2\theta}{x}$$

where θ was the experimental value obtained from a boundary-layer survey at a given station and x was the distance from the station to the virtual origin of the turbulent boundary layer.

RESULTS AND DISCUSSION

Skin-Friction Balance Data

Typical plots of basic experimental drag, in pounds, as measured by the balance are presented in figure 7 as a function of tunnel stagnation pressure for three of the five stations. As previously stated, the four available balances were interchanged among the five stations during the test program. All four balances were not necessarily used at any one station. Each symbol represents a different balance.

Examination of figure 7 shows that the drag increased fairly rapidly at the lower pressure range and the drag curve tended to flatten out for a more linear increase at the higher range. Flagged values indicate good repeatability for an individual balance. There is, however, a discrepancy in the drag indications of the various balances. The difference in the drag indications is attributed to different amounts of leakage or flow around the balance disk. Inasmuch as there was no feasible way of measuring the amounts of leakage and correcting for this effect, or of knowing which balance yielded the more correct reading, a curve was faired through the experimental data points of all the balances. This curve was used in calculating the local skin-friction coefficients.

Values of drag from the faired curves of test data, similar to those of figure 7, were reduced to give the local skin-friction coefficients at Mach numbers 1.61 and 2.20 that are presented in figure 8(a) as a function of Reynolds number per foot, and in figure 8(b) as a function of x' (distance to the tunnel first minimum). For convenience, a 1/5-slope line has been included in each set of experimental data to aid in comparing slopes and levels of experimental data.

For the set of data plotted as the variation of local skin-friction coefficient with Reynolds number per foot, the data for each station generally fall on separate curves which approximate straight lines. As expected, the local skin-friction coefficients decreased with increase in pressure.

For the plots of local skin-friction coefficient against x' (station distance to the tunnel first minimum), the rate of decrease in local skin-friction coefficient with increase in the downstream location is greater than one-fifth, the larger rate of change being at Mach number 2.20. The amount of scatter in the data appears to be effectively greater when the data are plotted as a function of x' than when they are plotted as a function of Reynolds number per foot.

Boundary-Layer Momentum Survey Data

Plots of typical experimental profiles obtained in this investigation are presented in figure 9. To assure clarity of the figure, only a portion of the experimental data at each Reynolds number per foot is shown. The figure indicates that an adequate number of points were taken to define the

velocity-profile shape. Data similar to these were reduced to give the computed values of momentum thickness θ presented in figure 10(a) as a function of Reynolds number per foot and in figure 10(b) as a function of x' (distance to tunnel first minimum). It may be noted that in some cases θ is an average of several repeated points. Generally, different values of θ at a station for repeat tunnel conditions agreed within 2 to 3 percent of one another but there were a few cases in which the θ values varied by as much as 6 to 10 percent of one another.

As in figure 8(a) a sloped line of arbitrary level has been included in figure 10(a) for comparison purposes. The data for the individual stations tend to vary linearly with Reynolds number per foot. Comparison of the data with the 1/5-slope line indicates that at Mach number 1.61 the slope of the data curve is less than one-fifth. At Mach number 2.20 the slopes of the data curves for the individual stations match approximately the 1/5-slope line.

Plots of θ as a function of x' follow the expected trend of an increase in θ with an increase in station downstream location. At the higher Mach number, θ increases more rapidly with change in the downstream location.

Average and Local Skin-Friction Coefficients

Experimental average skin-friction coefficients and local skin-friction coefficients as functions of Reynolds number based on free-stream conditions and the distance to the virtual origin of the turbulent boundary layer R_x are presented in figures 11 and 12. Included in the upper half of each figure are five of the more reliable theories or empirical formulas for comparison with the experimental data. (See refs. 3 to 9.) The data indicate that the effective Reynolds number range is from about 7×10^6 to 150×10^6 at Mach numbers of 1.61 and 2.20. In general, the experimental C_F data are in agreement with the level of these theories although the averages of the experimental data tend to lie above the theoretical predictions at Mach number 1.61 and below the theoretical predictions at Mach number 2.20. Since the experimental data exhibit more scatter than was hoped for, the accuracy is insufficient to warrant any conclusion as to which theory agrees best with the experimental data at these high Reynolds numbers. Most of the experimental data do however indicate that the variation of C_F with R_x at these high Reynolds numbers will tend to follow the theoretical predictions.

Experimental C_f as a function of R_x are presented in the lower half of figures 11 and 12. Since any one of the theories included in the upper portion of figures 11 and 12 could be said to be representative of the others, only one T' curve is presented. The experimental C_f data appear to be in better agreement with the Sommer and Short T' method (and hence with the other theories it represents) than the experimental average skin-friction data are with the theory. This effect probably can be attributed to the fact that the average skin-friction coefficient is inversely proportional to the distance from the virtual origin whereas the local skin-friction coefficient is based

on the local shear and free-stream conditions outside the boundary layer and therefore is independent of the location of the virtual origin.

Examination of the experimental skin-friction coefficients indicates that there was a different virtual origin for each data point. Although the virtual origin of the turbulent boundary layer may vary with variation of tunnel pressure, it does not seem likely that there should be a variation of virtual origin for each station at a constant pressure.

To correct for this incompatibility, average values of virtual origin were calculated for each constant pressure. These calculations, in terms of distance from the tunnel first minimum are presented in figure 13 as a function of tunnel stagnation pressure. For $M = 2.20$, there was essentially no change except for random scatter, whereas at $M = 1.61$ at the lower pressures there is a rapid downstream shift. Average skin-friction coefficients and effective Reynolds numbers were then reduced to this new virtual origin. These results are presented in figures 14 and 15. Short dashed lines have been faired through the station data obtained at a constant tunnel pressure. Sommer and Short T' theory curves have been included in the figures for comparison. Under the new set of restrictions on the virtual origin, the average skin-friction coefficient C_F as derived from the momentum surveys, actually increases with downstream distance. Conversely, the local skin-friction coefficient C_f, obtained from the friction-balance readings, decreases too rapidly with increase in distance. These results thus tend to imply that the boundary-layer flow on the tunnel wall is not two dimensional. Because of restrictions on cutting holes in flexible nozzle walls, the tests were made on the sidewalls. Hence, the boundary layer from the first minimum must traverse a longer path and be immersed in the lower Mach number flow for a greater distance at the top and bottom of the wall than along the wall center line before reaching the measuring stations. (See fig. 3.) The boundary-layer momentum thickness should therefore be minimum at the tunnel center line and increase toward the top and bottom of the wall. Consequently, because of boundary-layer cross-flow effects the momentum surveys will indicate too rapid an increase in momentum thickness, and the thicker boundary layer will result in too rapid a decrease in C_f with increasing x, particularly if the flow expansion is not perfectly symmetric with respect to the wall center line. This variation is shown more clearly in figure 16 where increase in drag is plotted as a function of increase in surface distance from the tunnel first minimum, as derived from the momentum survey and the skin-friction balance data. In order to adjust the local skin-friction drag data to the average skin-friction drag data, it was assumed that the value of drag measured by the skin-friction balance of station 1 was the same as the drag value measured by the momentum survey at the same station. Generally, the growth in momentum-survey data is faster than the growth in skin-friction balance data for the same x' distance.

CONCLUSIONS

An investigation has been made to gather experimental skin-friction data over a wide range of high Reynolds numbers at low supersonic velocities. Tests were conducted at Mach numbers of 1.61 and 2.20 over a range of tunnel Reynolds number per foot from about 0.8×10^6 to 8.0×10^6. The results indicate that:

1. The effective Reynolds number range based on distances reduced to a virtual origin is from about 7×10^6 to 150×10^6 at Mach numbers of 1.61 and 2.20.

2. Experimental average skin-friction coefficients and experimental local skin-friction coefficients for the range of Reynolds number from about 7×10^6 to 150×10^6 are in agreement with the levels of the Sommer and Short T', the Monaghan T', the Eckert T', the Cope and Monaghan, the Wilson and Van Driest theoretical or theoretical-empirical curves, and variations of skin-friction coefficients with effective Reynolds number tend to follow the theoretical predictions.

Langley Research Center,
National Aeronautics and Space Administration,
Langley Station, Hampton, Va., November 16, 1964.

REFERENCES

1. Shutts, W. H.; Hartwig, W. H.; and Weiler, J. E.: Final Report on Turbulent Boundary-Layer and Skin-Friction Measurements on a Smooth, Thermally Insulated Flat Plate at Supersonic Speeds. DRL-364, CM-823 (Contract NOrd-9195), Univ. of Texas, Jan. 5, 1955.

2. Peterson, John B., Jr.: A Comparison of Experimental and Theoretical Results for the Compressible Turbulent-Boundary-Layer Skin Friction With Zero Pressure Gradient. NASA TN D-1795, 1963.

3. Sommer, Simon C.; and Short, Barbara J.: Free-Flight Measurements of Turbulent-Boundary-Layer Skin Friction in the Presence of Severe Aerodynamic Heating at Mach Numbers From 2.8 to 7.0. NACA TN 3391, 1955.

4. Cope, W. F.: The Turbulent Boundary Layer in Compressible Flow. R. & M. No. 2840, Brit. A.R.C., 1953.

5. Monaghan, R. J.; and Johnson, J. E.: The Measurement of Heat Transfer and Skin Friction at Supersonic Speeds. Part II - Boundary Layer Measurements on a Flat Plate at $M = 2.5$ and Zero Heat Transfer. C.P. No. 64, Brit. A.R.C., 1952.

6. Monaghan, R. J.: On the Behavior of Boundary Layers at Supersonic Speeds. Fifth International Aeronautical Conference (Los Angeles, Calif., June 20-23, 1955), Inst. Aero. Sci., Inc., 1955, pp. 277-315.

7. Eckert, Ernst R. G.: Survey on Heat Transfer at High Speeds. WADC Tech. Rept. 54-70, U.S. Air Force, Apr. 1954.

8. Van Driest, E. R.: Turbulent Boundary Layer in Compressible Fluids. J. Aeron. Sci., vol. 18, no. 3, Mar. 1951, pp. 145-160, 216.

9. Wilson, R. E.: Turbulent Boundary-Layer Characteristics at Supersonic Speeds - Theory and Experiment. J. Aeron. Sci., vol. 17, no. 9, Sept. 1950, pp. 585-594.

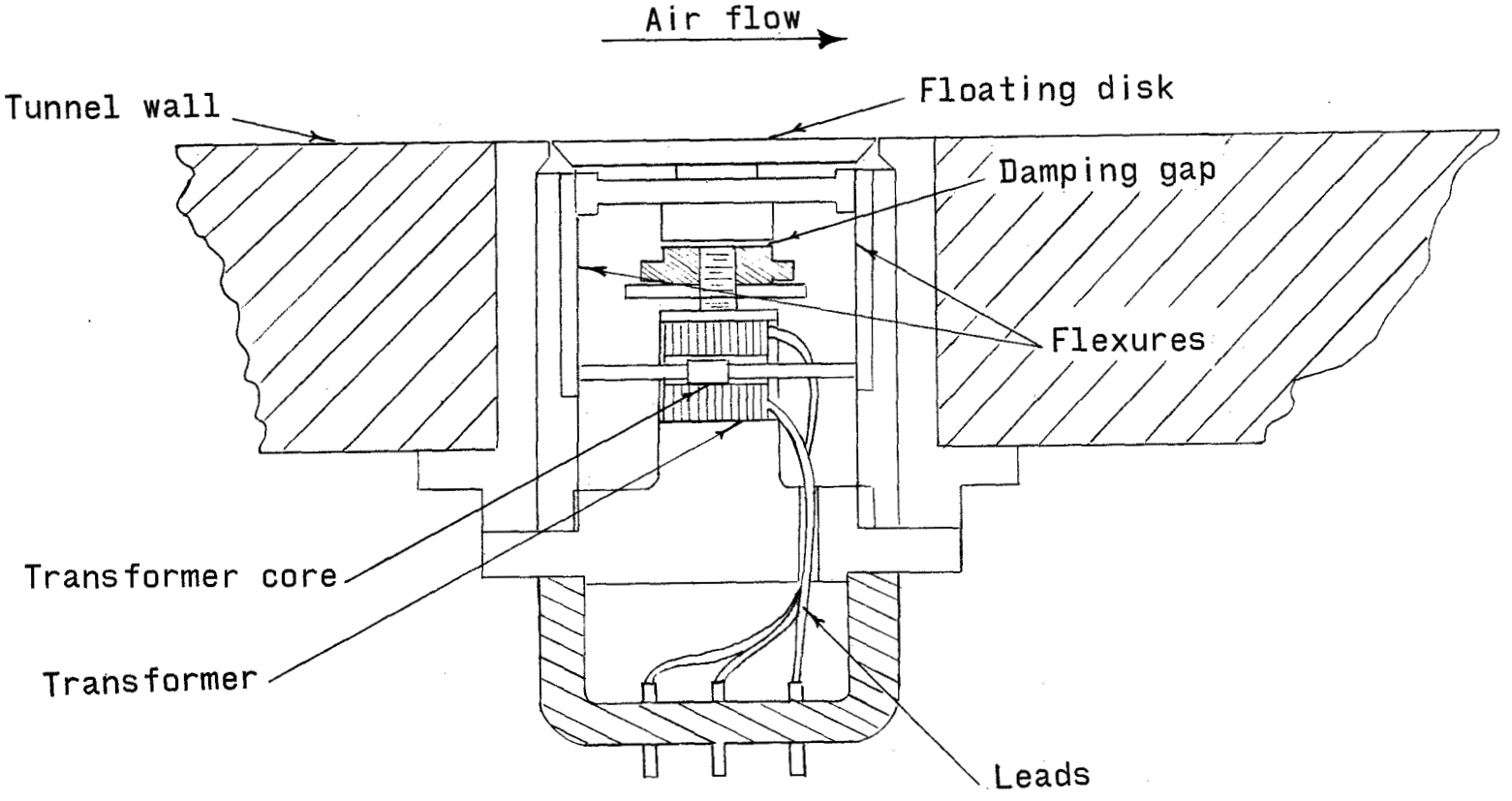

Figure 1.- Schematic drawing of a typical floating-element balance.

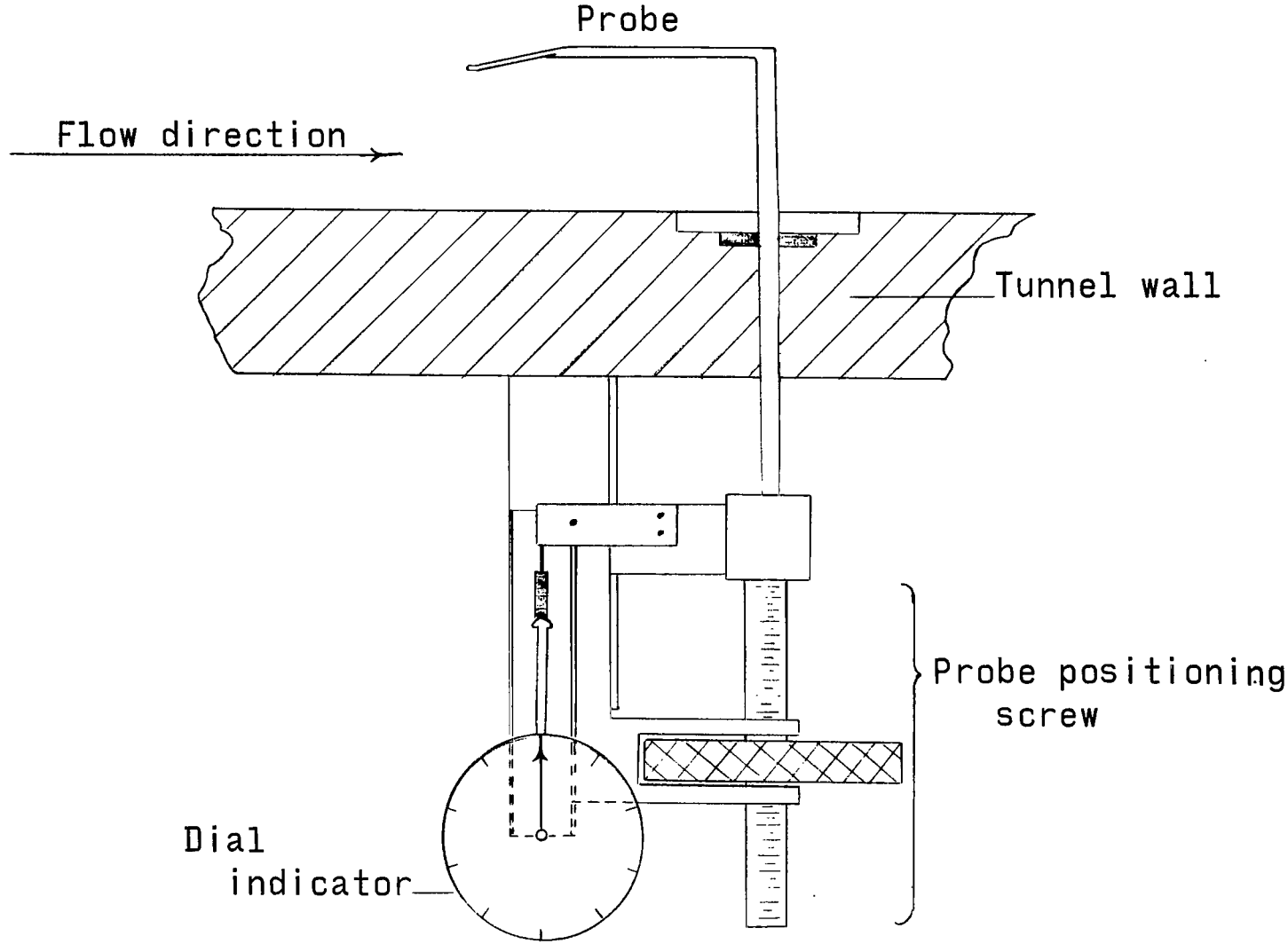

Figure 2.- Boundary-layer probe and mechanism.

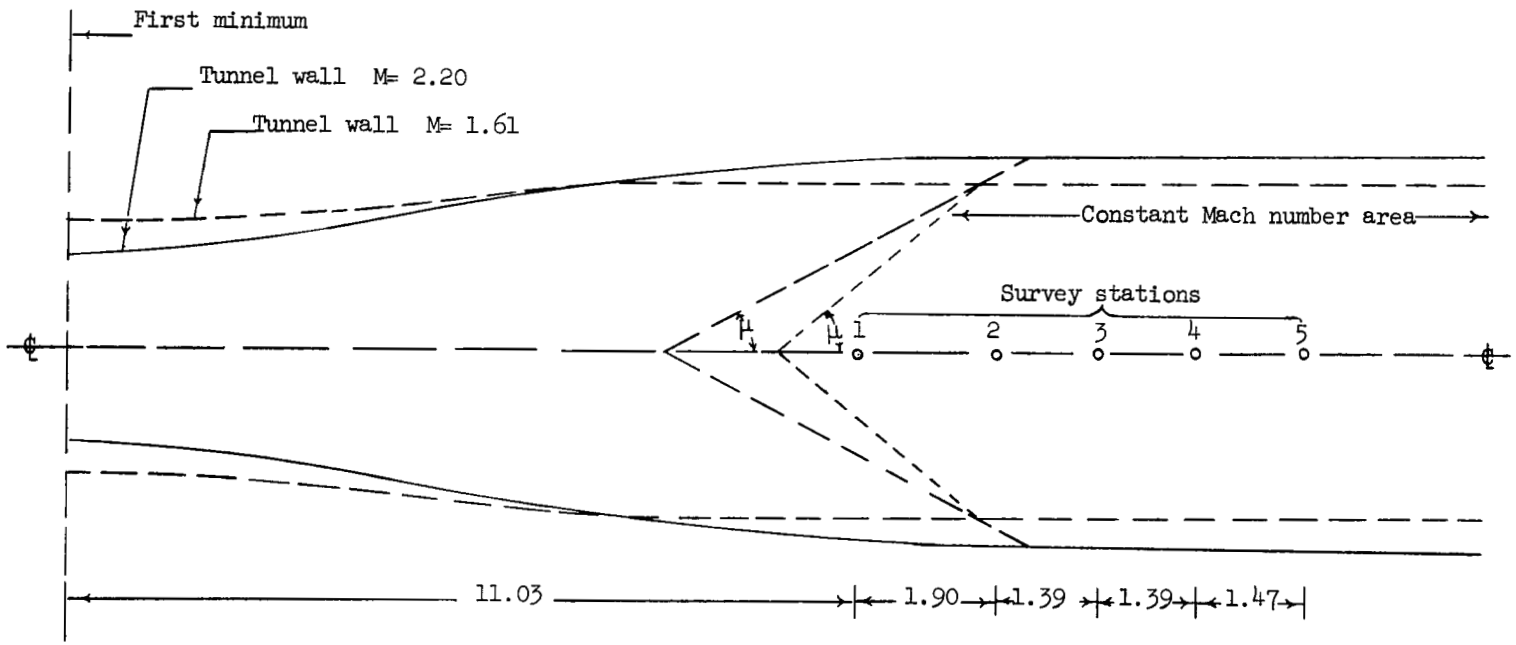

Figure 3.- Nominal locations of balance and momentum stations. All dimensions are in feet.

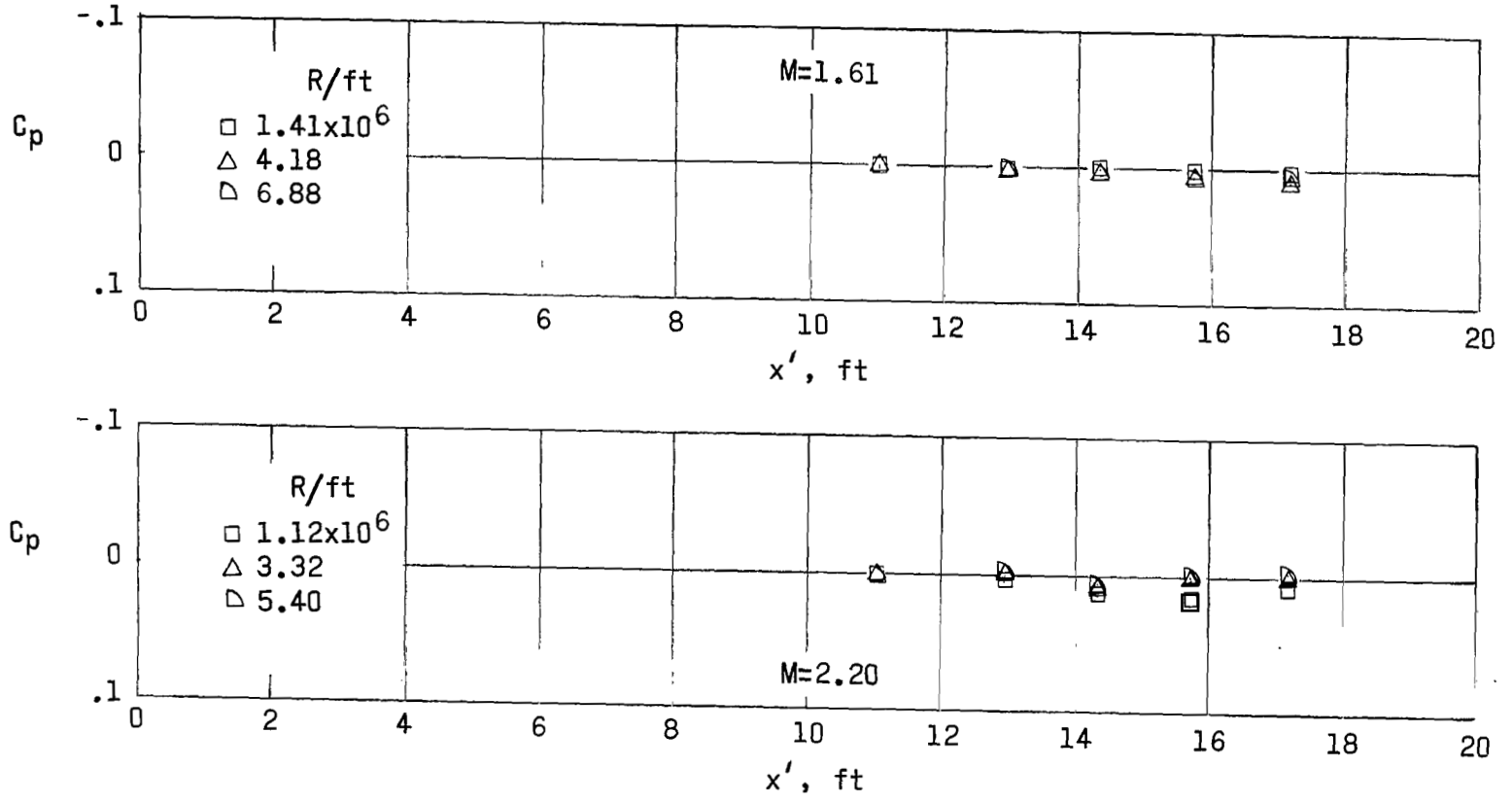

Figure 4.- Typical experimental C_p measured at wall-survey stations as a function of x' (distance from tunnel first minimum).

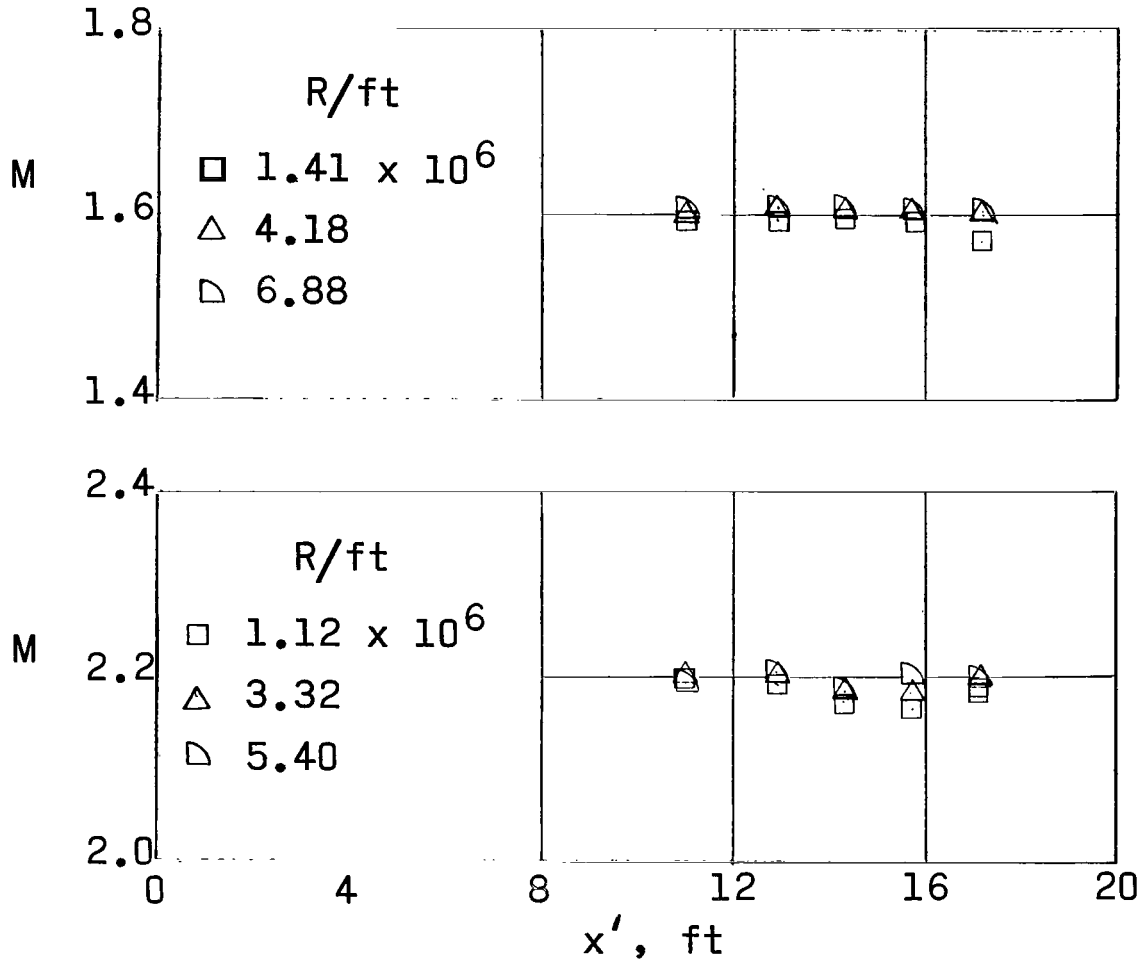

Figure 5.- Mach number based on $p/p_{t,1}$ as a function of x'.

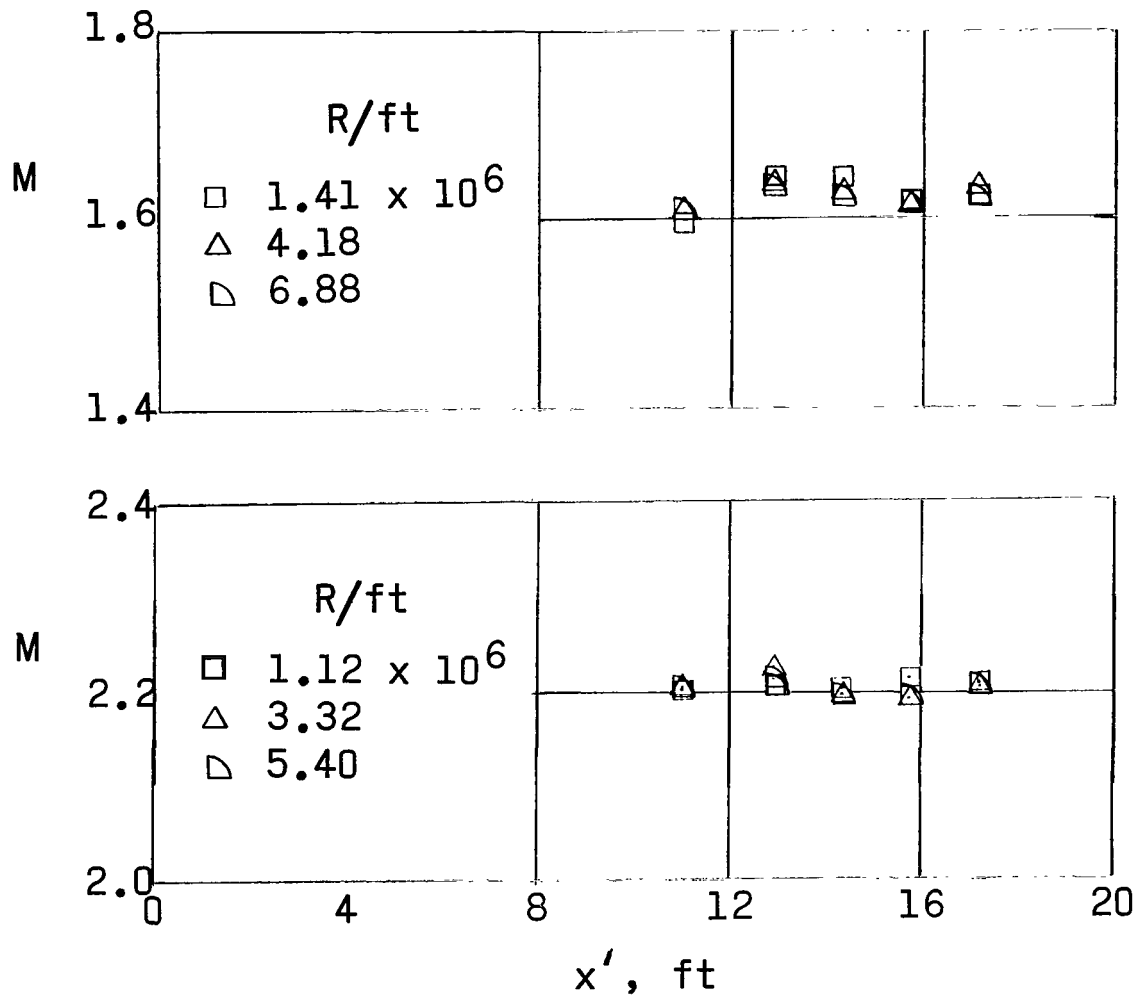

Figure 6.- Mach number based on $p_{t,2}/p_{t,1}$ as a function of x'.

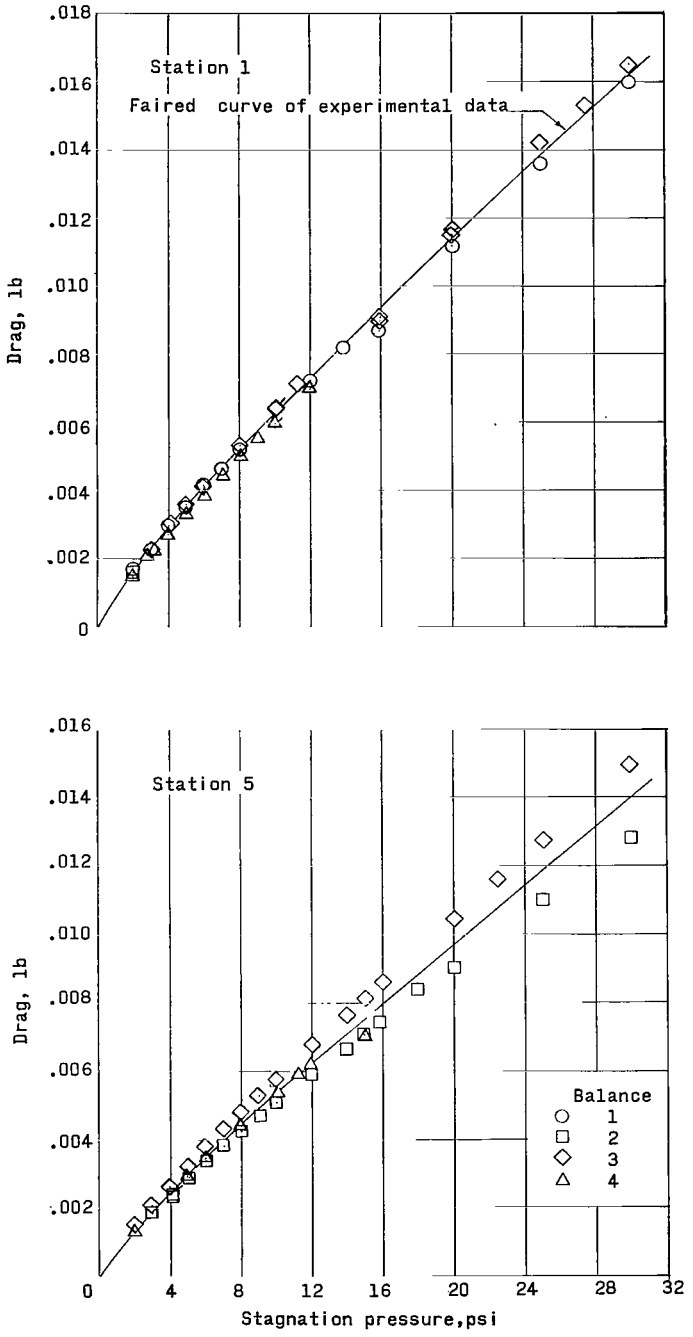

(a) M = 1.61.

Figure 7.- Typical experimental local skin-friction drag as a function of tunnel stagnation pressure.

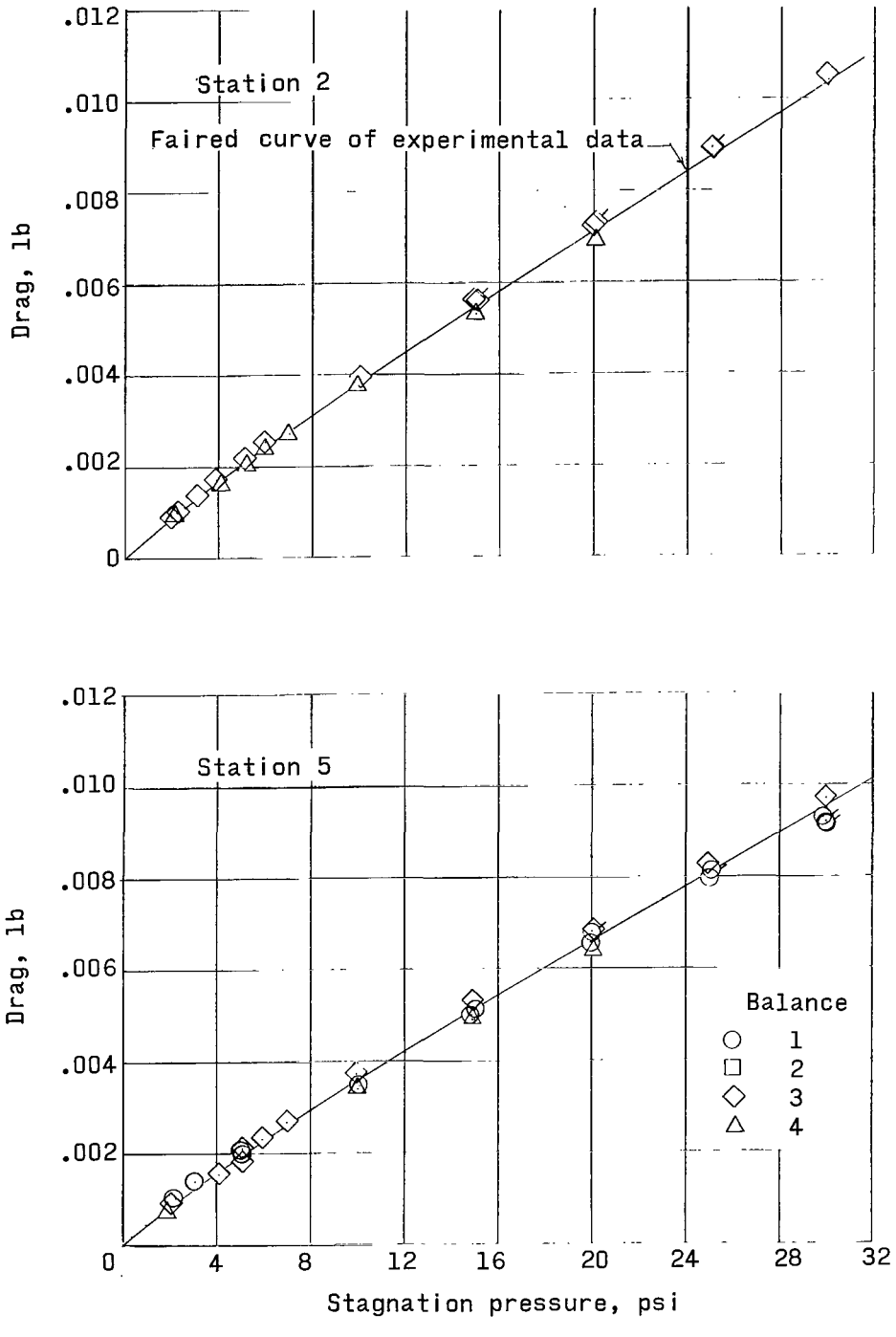

(b) M = 2.20.

Figure 7.- Concluded.

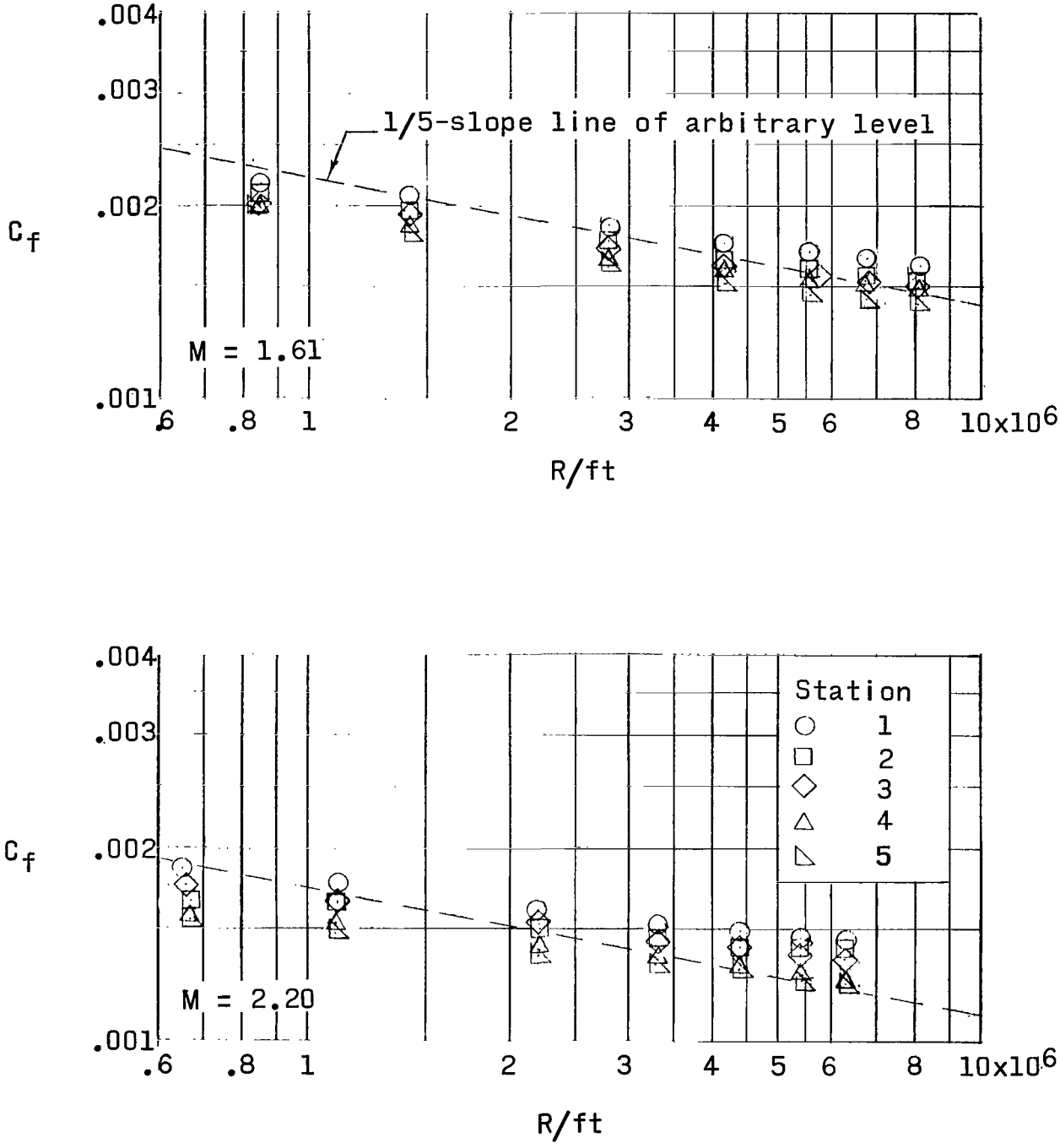

(a) As a function of Reynolds number per foot.

Figure 8.- Experimental local skin-friction coefficients.

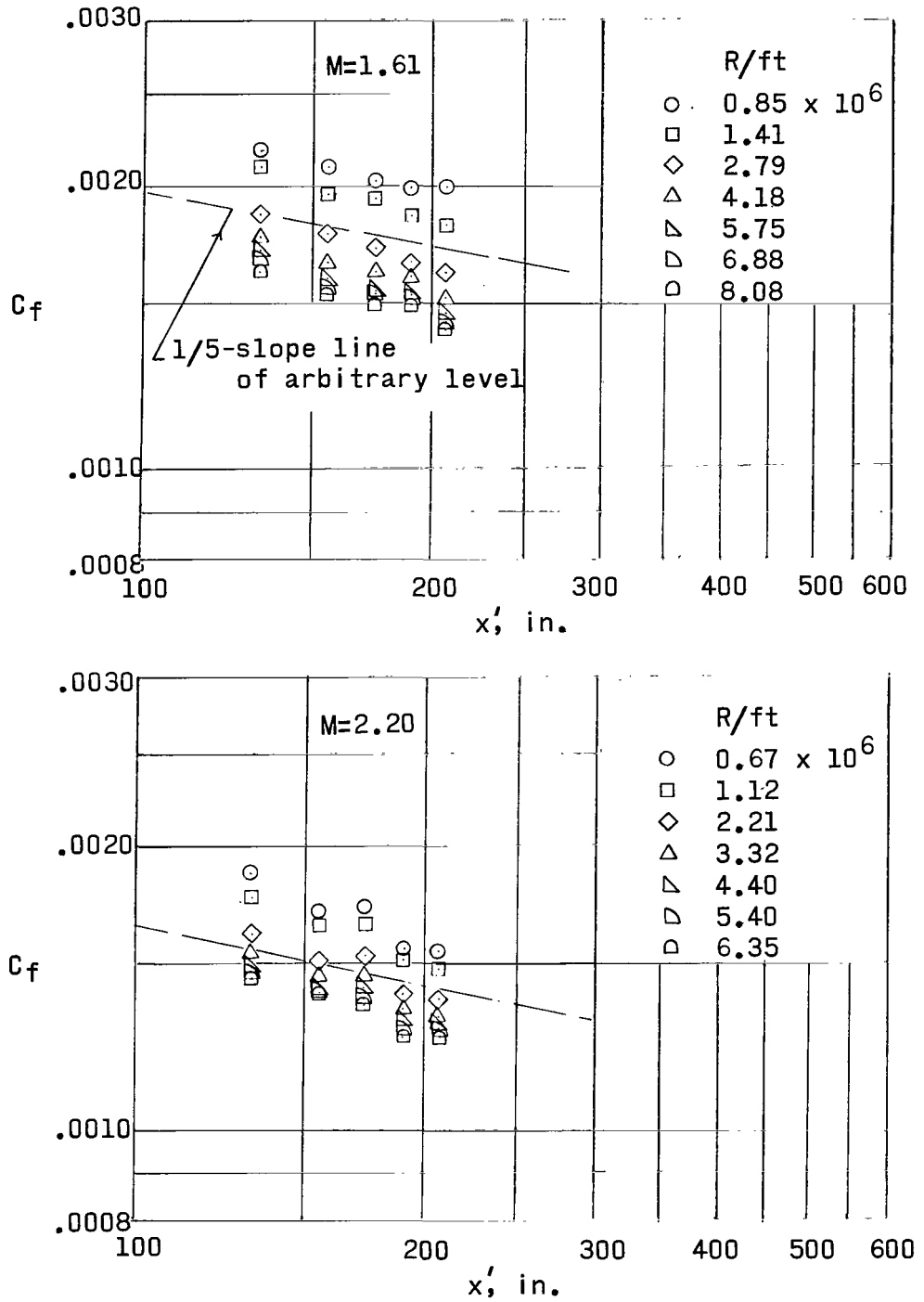

(b) As a function of x' (distance from tunnel first minimum).

Figure 8.- Concluded.

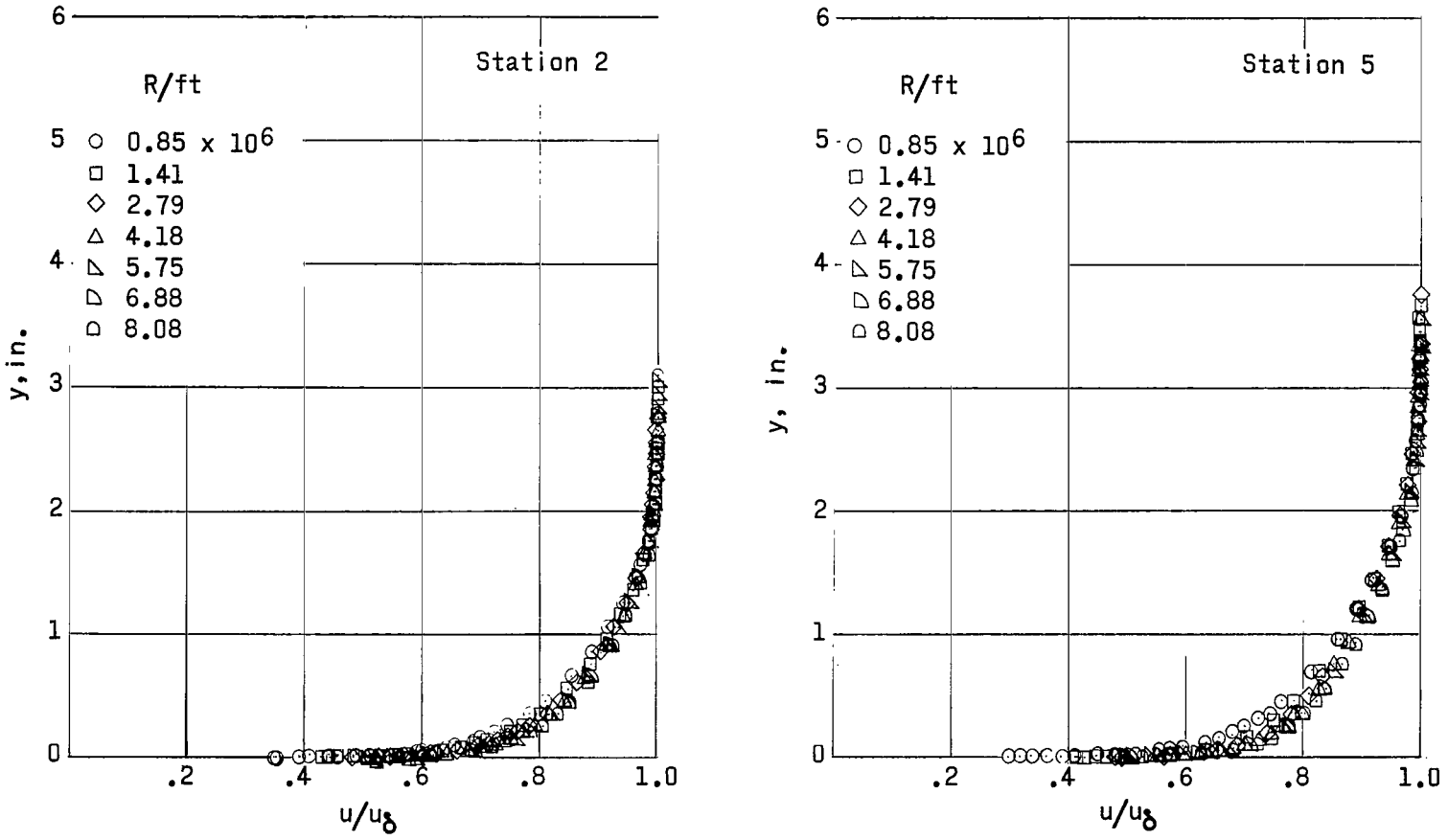

(a) M = 1.61.

Figure 9.- Typical experimental velocity profiles.

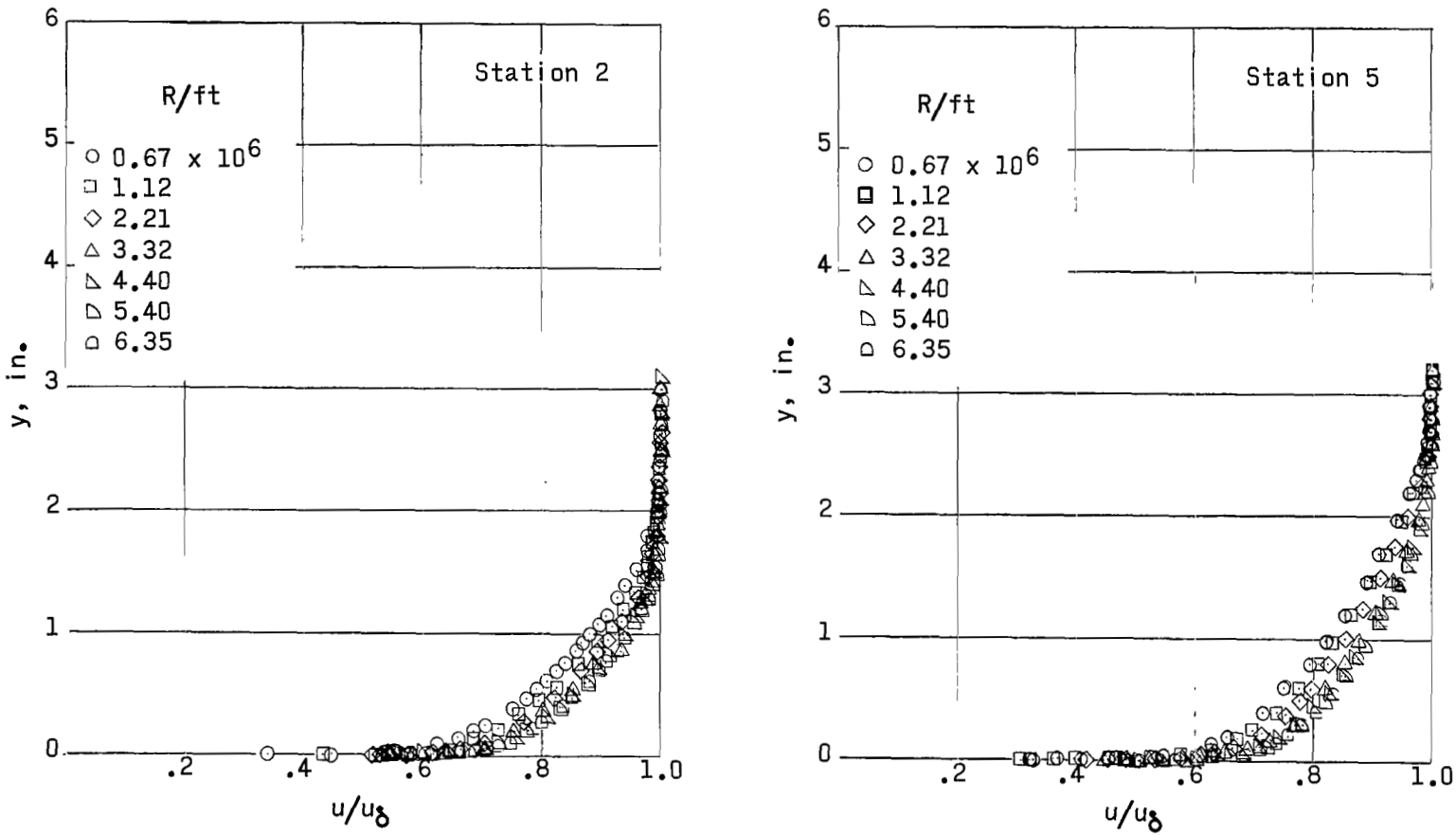

(b) M = 2.20.

Figure 9.- Concluded.

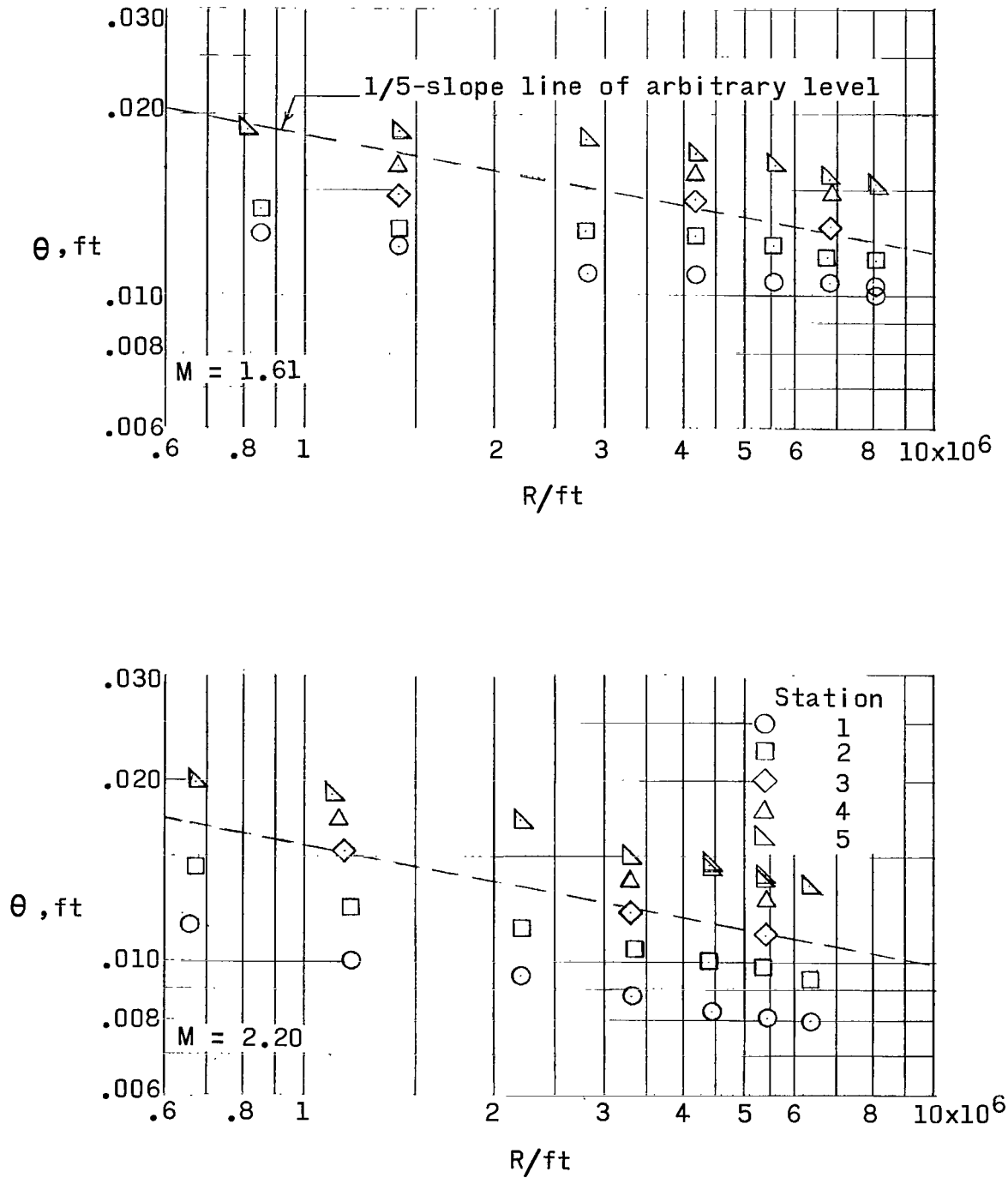

(a) As a function of Reynolds number per foot.

Figure 10.- Experimental momentum thickness.

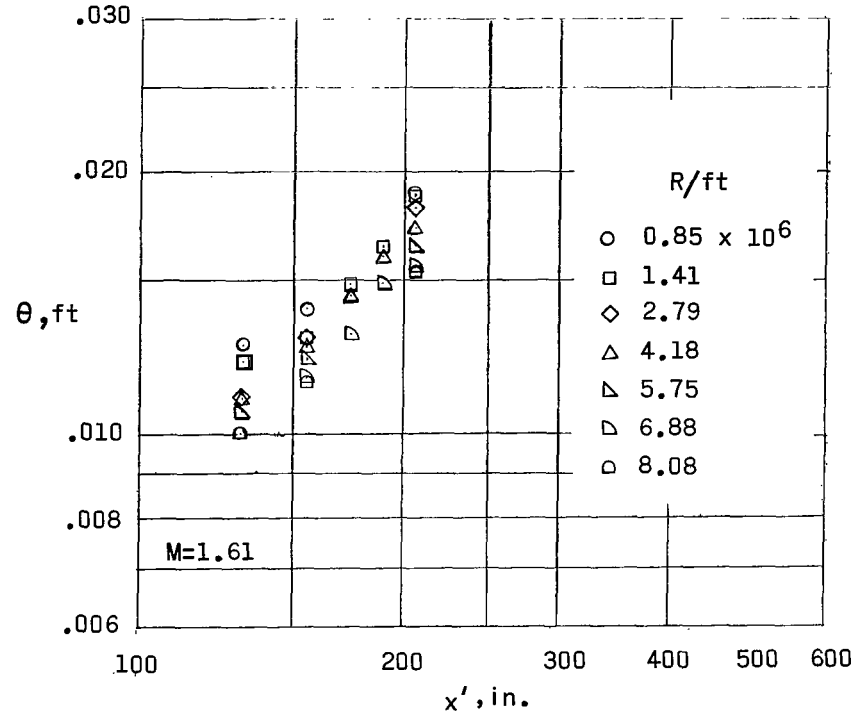

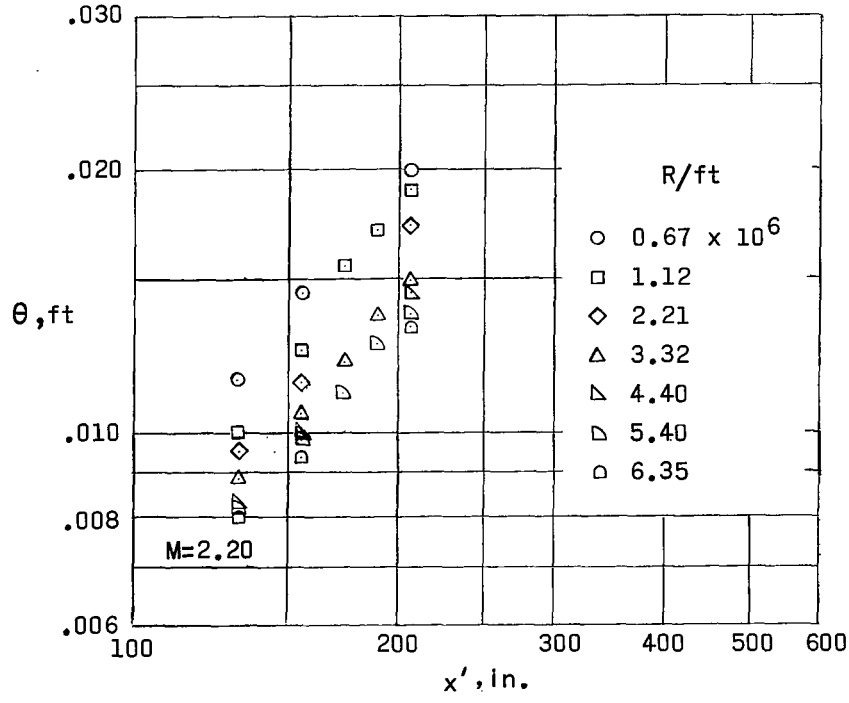

(b) As a function of x' (distance from tunnel first minimum).

Figure 10.- Concluded.

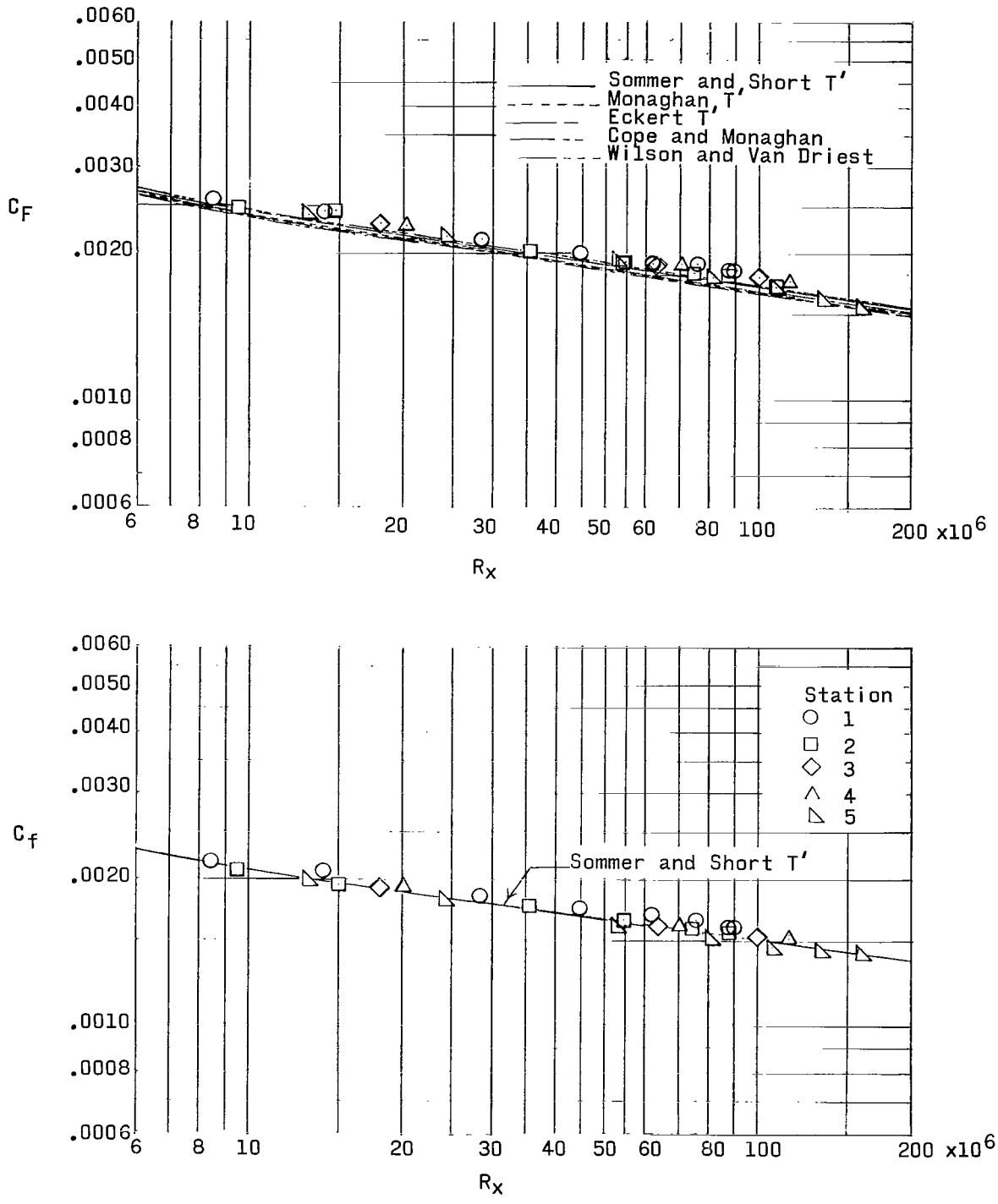

Figure 11.- Experimental skin-friction coefficients as a function of R_x. M = 1.61; variable virtual origin.

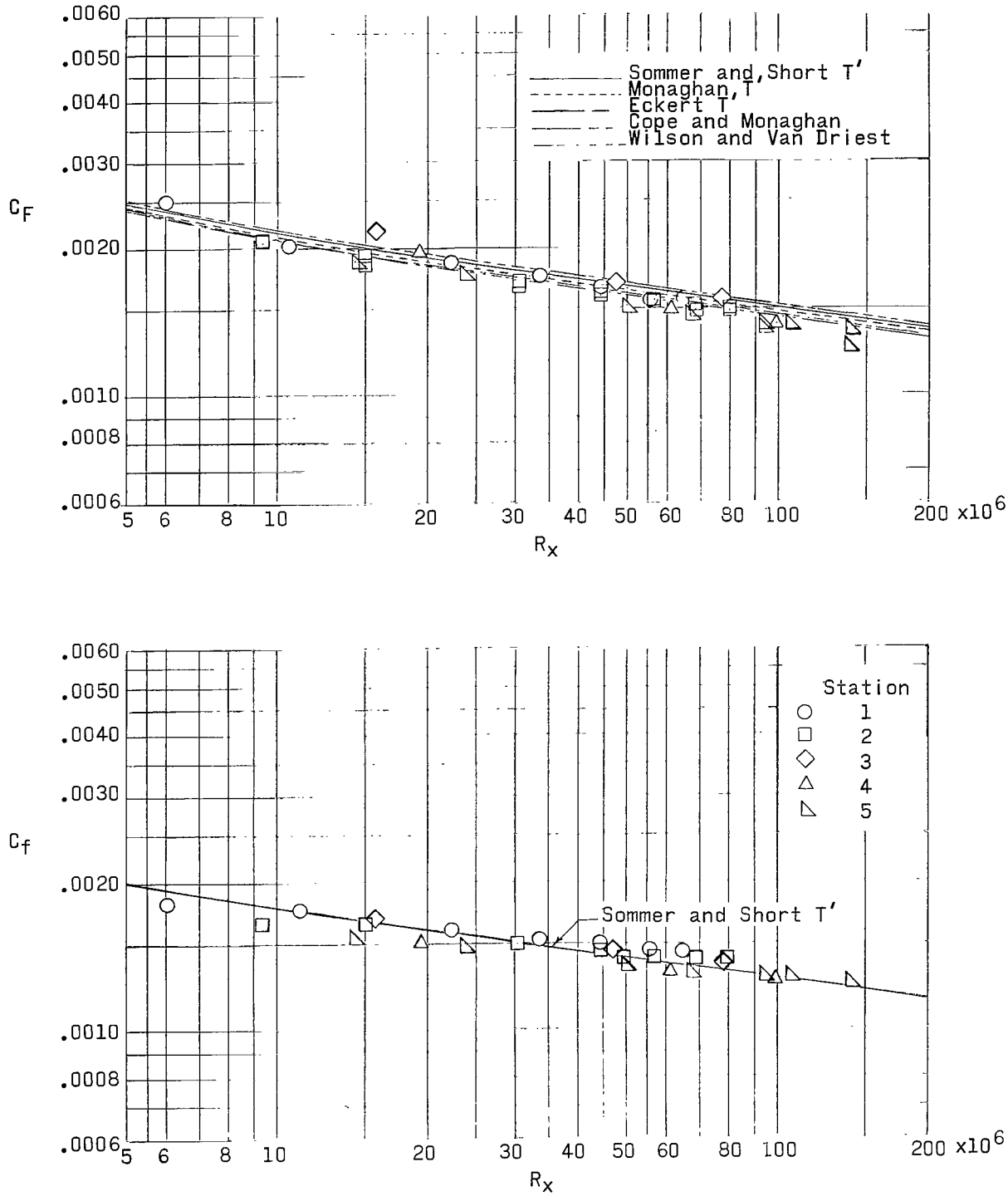

Figure 12.- Experimental skin-friction coefficients as a function of R_x. M = 2.20; variable virtual origin.

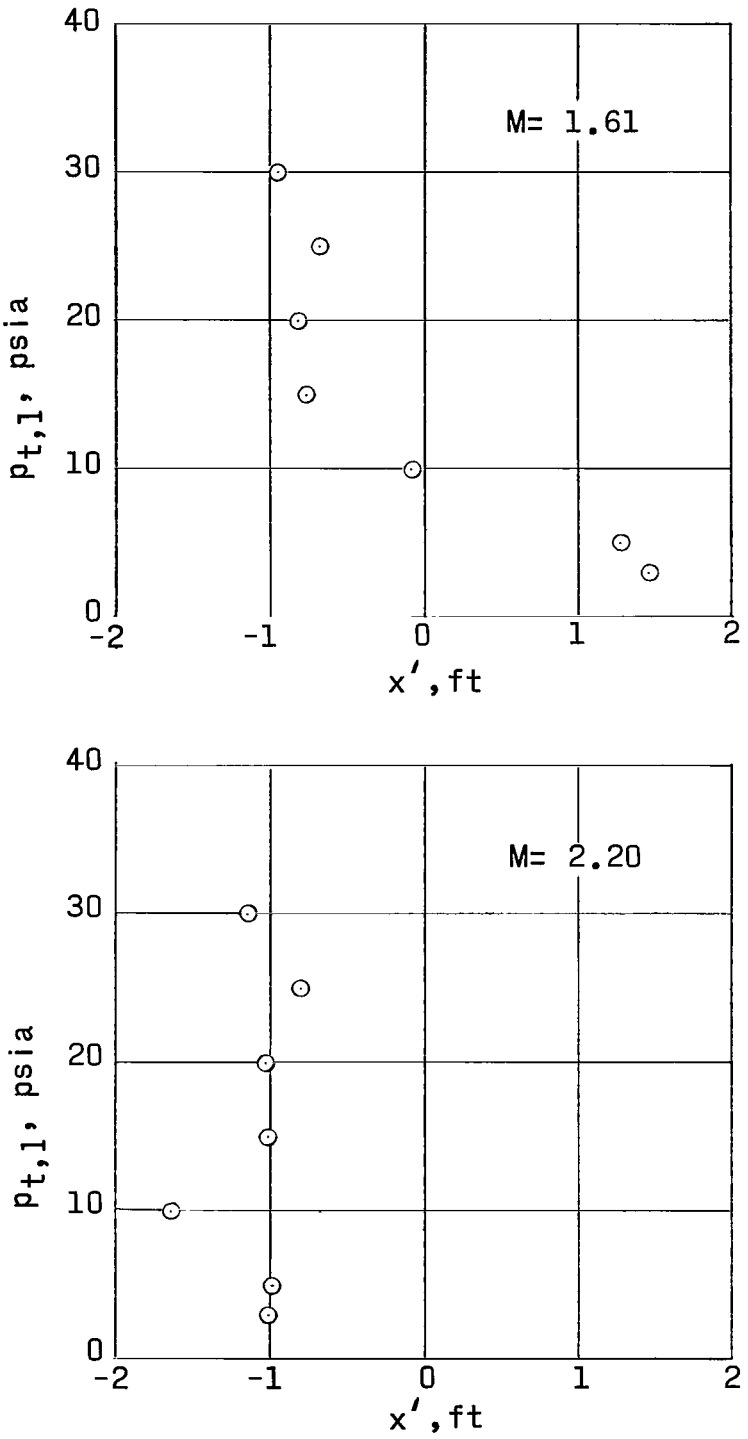

Figure 13.- Location of virtual origin as a function of tunnel stagnation pressure.

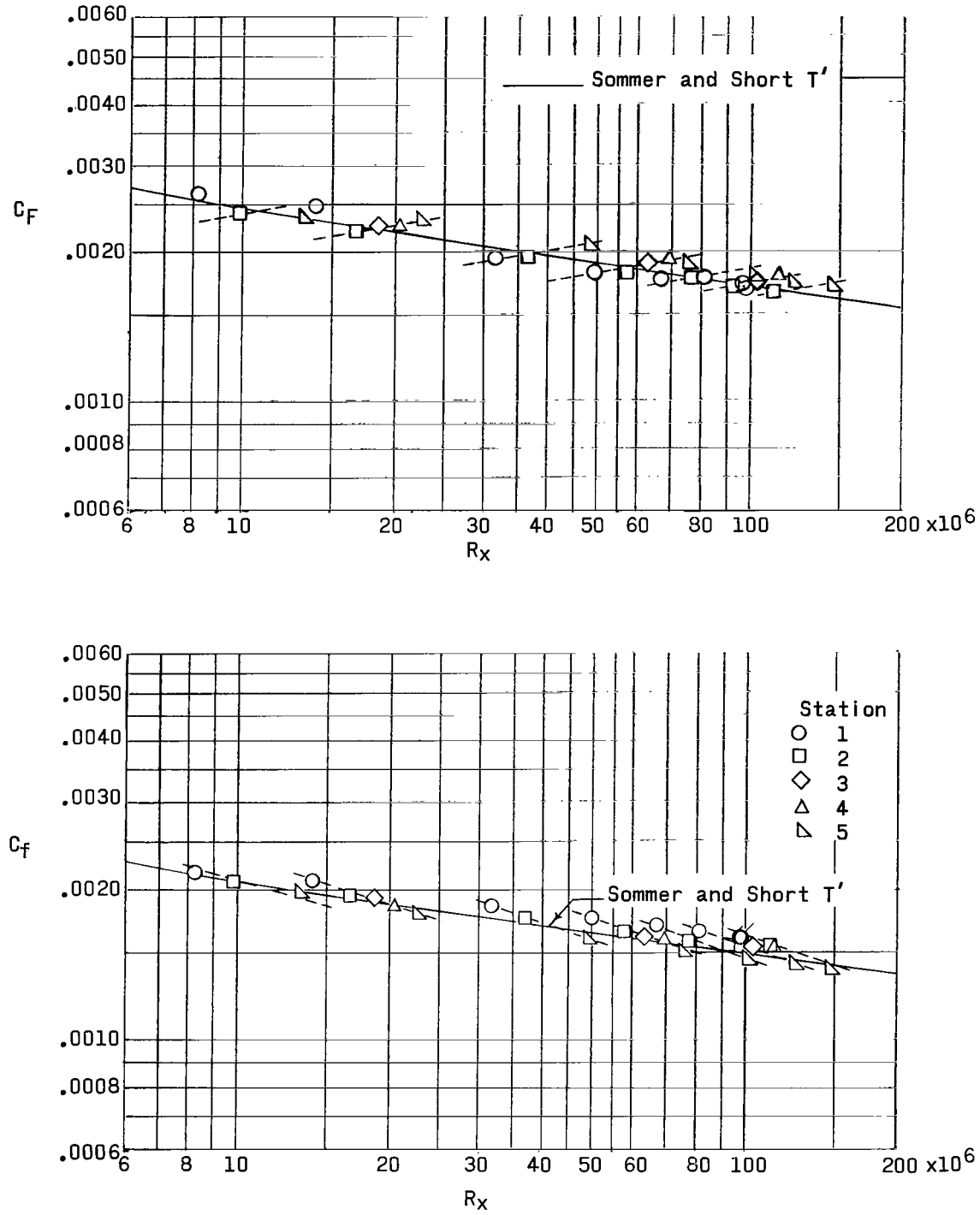

Figure 14.- Experimental skin-friction coefficients as functions of R_x. Short dashed lines are fairings of data at constant pressure. M = 1.61; constant virtual origin.

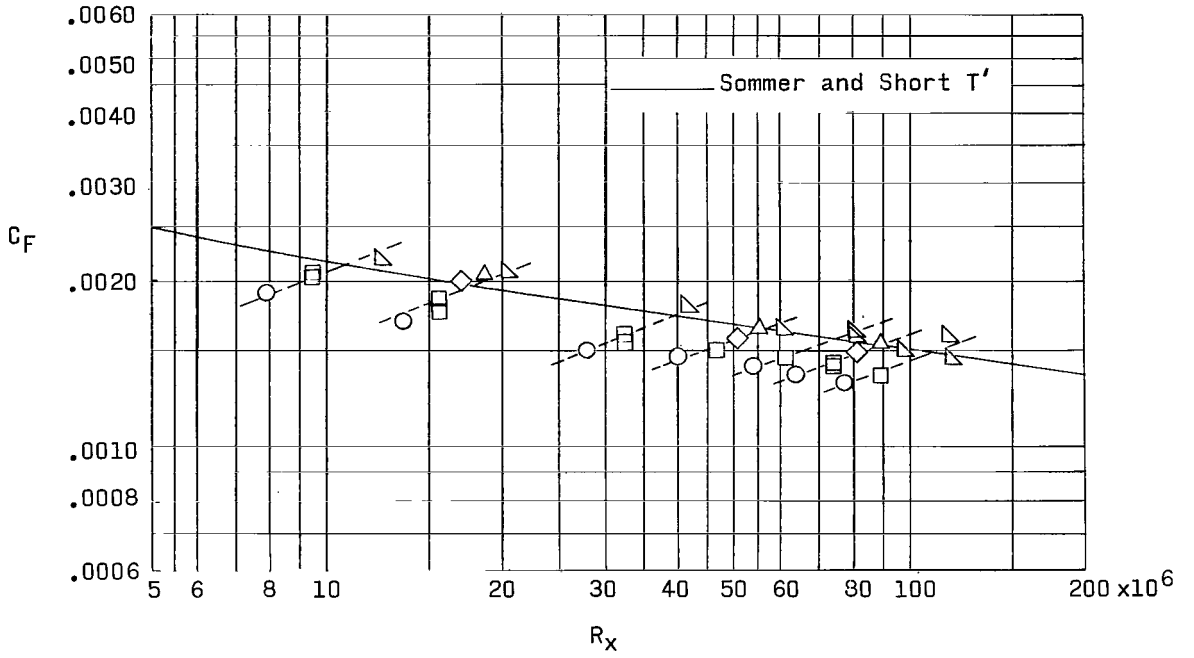

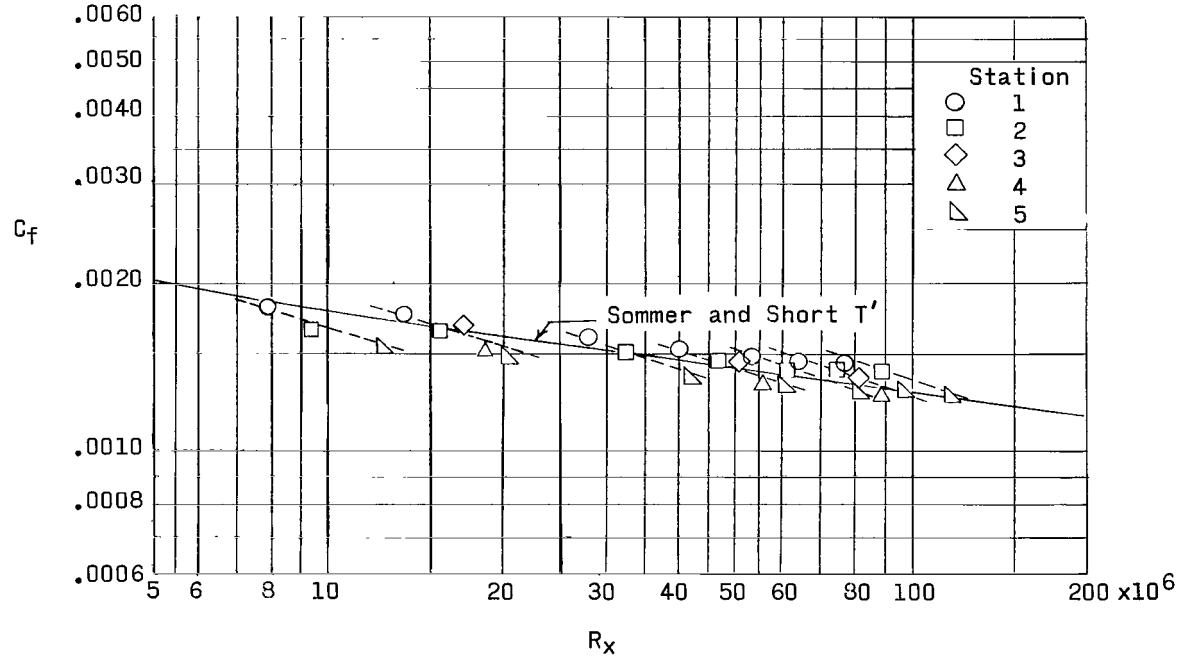

Figure 15.- Experimental skin-friction coefficients as functions of R_x. Short dashed lines are fairings of data at constant pressure. M = 2.20; constant virtual origin.

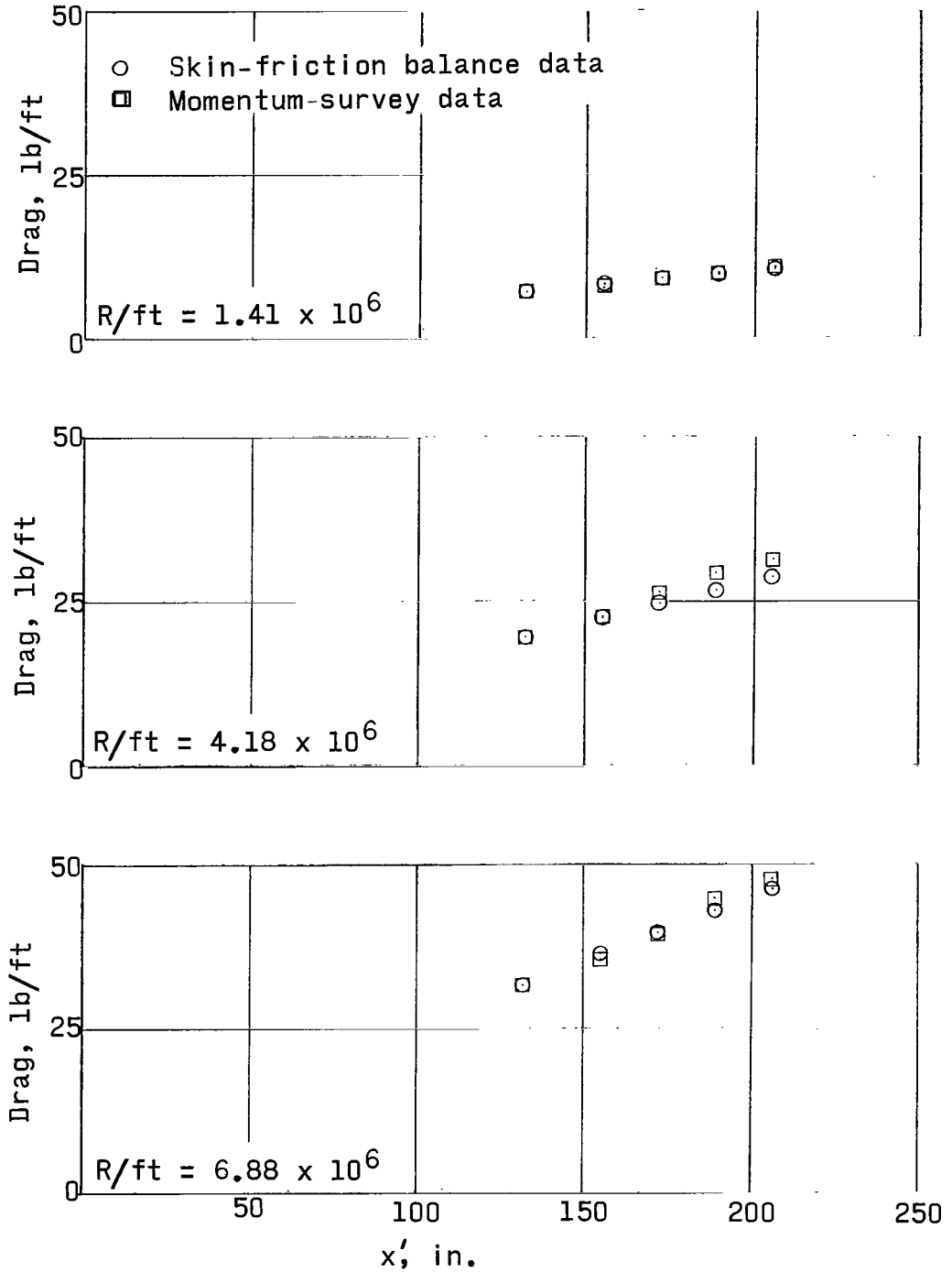

(a) M = 1.61.

Figure 16.- Comparison of skin-friction balance and momentum-survey data on basis of drag.

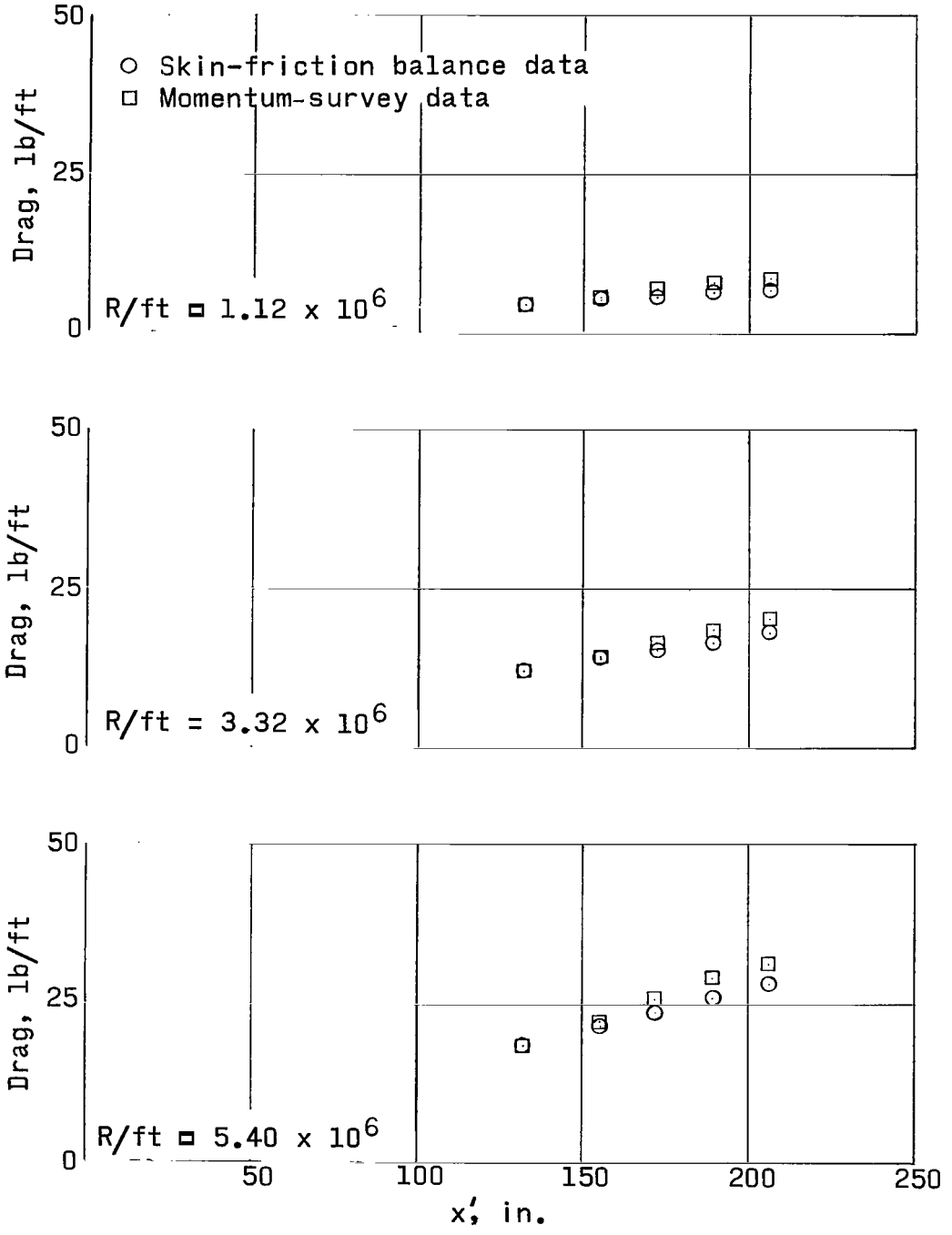

(b) M = 2.20.

Figure 16.- Concluded.

"The aeronautical and space activities of the United States shall be conducted so as to contribute . . . to the expansion of human knowledge of phenomena in the atmosphere and space. The Administration shall provide for the widest practicable and appropriate dissemination of information concerning its activities and the results thereof."

—NATIONAL AERONAUTICS AND SPACE ACT OF 1958

NASA SCIENTIFIC AND TECHNICAL PUBLICATIONS

TECHNICAL REPORTS: Scientific and technical information considered important, complete, and a lasting contribution to existing knowledge.

TECHNICAL NOTES: Information less broad in scope but nevertheless of importance as a contribution to existing knowledge.

TECHNICAL MEMORANDUMS: Information receiving limited distribution because of preliminary data, security classification, or other reasons.

CONTRACTOR REPORTS: Technical information generated in connection with a NASA contract or grant and released under NASA auspices.

TECHNICAL TRANSLATIONS: Information published in a foreign language considered to merit NASA distribution in English.

TECHNICAL REPRINTS: Information derived from NASA activities and initially published in the form of journal articles.

SPECIAL PUBLICATIONS: Information derived from or of value to NASA activities but not necessarily reporting the results of individual NASA-programmed scientific efforts. Publications include conference proceedings, monographs, data compilations, handbooks, sourcebooks, and special bibliographies.

Details on the availability of these publications may be obtained from:

SCIENTIFIC AND TECHNICAL INFORMATION DIVISION

NATIONAL AERONAUTICS AND SPACE ADMINISTRATION

Washington, D.C. 20546